IEEE Access
Multidisciplinary | Rapid Review | Open Access Journal

Received February 13, 2020, accepted March 29, 2020, date of publication April 7, 2020, date of current version May 1, 2020.

Digital Object Identifier 10.1109/ACCESS.2020.2986349

Energy Efficient Full-Duplex UAV Relaying Networks Under Load-Carry-and-Delivery Scheme

NAN QI[1], (Member, IEEE), MEI WANG[1], WEN-JING WANG[2], (Member, IEEE), THEODOROS A. TSIFTSIS[3,4], (Senior Member, IEEE), RUGUI YAO[5], (Senior Member, IEEE), AND GUANGHUA YANG[3,4], (Senior Member, IEEE)

[1]Key Laboratory of Dynamic Cognitive System of Electromagnetic Spectrum Space, Ministry of Industry and Information Technology, Nanjing University of Aeronautics and Astronautics, Nanjing 210016, China
[2]School of Communication and Information Engineering, Xi'an University of Posts and Telecommunications, Xi'an 710121, China
[3]Institute of Physical Internet, Jinan University, Zhuhai 519070, China
[4]School of Intelligent Systems Science and Engineering, Jinan University, Zhuhai 519070, China
[5]School of Electronics and Information, Northwestern Polytechnical University, China

Corresponding author: Wen-Jing Wang (wjing@uvic.ca)

This work was supported in part by the National Natural Science Foundation of China under Grant 61801218 and Grant 61871327, in part by the Open Foundation for Graduate Innovation of NUAA under Grant kfjj20190417, in part by the Natural Science Foundation of Jiangsu Province under Grant BK20180424, and in part by the State Key Laboratory of Air Traffic Management System and Technology under Grant SKLATM201808.

ABSTRACT In this paper, an energy-efficient full-duplex (FD) unmanned aerial vehicle (UAV) relaying network is proposed, where UAV acts as a mobile relay and assists information exchange between two transceivers. Specifically, the load-carry-and-delivery scheme is applied to positively take advantage of the time-varying channel gain in delay-tolerant networks; meanwhile, the FD communication policy is used to potentially further increase the energy efficiency (EE). In particular, the self-interference channel gains follow the complex Gaussian distribution instead of being constant. The EE is first rigorously derived and then, the optimum flight speed is determined under the information causality constraint to maximize the EE. Numerical results demonstrate that the proposed scheme outperforms the half-duplex as well as static schemes in terms of the EE. In addition, the impact of the self-interference cancellation factor on the EE is also demonstrated, which provides valuable insights for the system design of UAV-assisted relaying networks.

INDEX TERMS Energy efficiency (EE), delay-tolerant networks, full-duplex relaying (FDR), load-carry-and-delivery (LCAD), UAV.

I. INTRODUCTION

Nowadays, commercial UAVs for various applications have been developed, including UAV for smart agriculture/forestry, security/fire monitoring and express transportation. As an emerging technique, UAV-integrated networks, have attracted significant considerations [1], [2], especially for dire or human hard-to-reach communication circumstances (i.e. fire brigades, earthquake-affected area, border detection, and remote sensing) due to their low-cost property, deployment flexibility, and intrinsic mobility. In particular, compared to terrestrial communication systems, UAV wireless systems bring new advantages, such as superior link quality of ground node (GNs) communication channels [2], and greater network flexibility with fully controllable flight trajectories in three-dimensional (3D) airspace [3]. UAVs-enabled communication is expected to improve cellular offloading for the overloaded base stations (BSs) and accelerate data collecting for the device-to-device (D2D) communications in the forthcoming 5G networks. The UAV relaying technique also finds its wide applications in assisting communication between two distant nodes [4]–[7]. *Fadel Adib* in MIT Media Lab builds UAV-based radio frequency identification devices (RFID) relay to track

The associate editor coordinating the review of this manuscript and approving it for publication was Yi Zhang.

boxes that dramatically extends the range of RFID, and could help retailers keep track of goods [5]. In [6], the authors investigated a UAV-relaying IoT scenario for sensor data collection. Therein, a relaying system was designed for environmental monitoring in agricultural applications. There are also some projects that provide Telemetry, Videolink over a selected area between ground station and UAV on mission [7].

Though UAV relaying transmission brings opportunities, it also encounters challenges. In practice, a UAV has a confined serving duration due to the practical size, weight, and on-board battery capacity. UAVs on the market today (e.g. DJI, Yuneec, and UVify) generally have a battery size of 2300-5400 mAh and flight duration of 5-30 minutes [8]–[10]. Achieving energy-efficient transmission is particularly urgent and critical in UAV-assisted networks. As a single metric, energy efficiency (EE) characterizes the amount of successfully transmitted bits per unit energy. In [11]–[13], energy-efficient terrestrial half-duplex relaying (HDR) transmissions were investigated, where the transmitting power was optimized. To effectively improve the energy efficiency for slotted transmission, the optimal slot length maximizing the energy efficiency is investigated in [13]. [14] and [15] focus on the UAV's trajectory design to maximize energy efficiency by taking the UAV's propulsion energy consumption into account. However, the above researches consider direct transmission scenarios. To improve the EE of aerial UAV relaying networks, except power management, two extra following methods are concluded [1], [4], [12], [16]–[18]. Firstly, carefully design the UAV flight behaviours (including flight duration and speed) when it executes a relaying mission [1], [12], [16], [17]. It is because UAV flight behaviours are closely related with the flight energy consumption which accounts for the very great proportion in overall energy consumption. Propulsion energy consumptions can be reduced with appropriate flight behaviours improvement. Secondly, schedule the data transmissions [4], [18]. This benefits from the fact that UAV is able to be adapted to the varying channel gains due to its intrinsic nature, which allows the received messages to be stored and forwarded until the UAV moves to an area with a higher better channel gain.

UAV half-duplex relaying (HDR) has been widely investigated [4], [17], [19] and [20]. A joint trajectory and power optimization was performed in [17] and [19] to respectively maximize the network throughput. Instead of throughput, in [20], the authors focus on maximizing the energy efficiency for UAV-HDR network that employs circular UAV trajectory and time-division duplexing (TDD). Compared with the full-duplex relaying (FDR) scheme, HDR consumes longer time duration to complete transmission. Scanning the open literature, the throughput of FDR networks have been proved to outperform that of the half-duplex scheme in some communication scenario (i.e. higher channel gains, lower self-interference (SI)) [21]–[23]. However, they mainly focus on the terrestrial relays (i.e. static relays). In [24], the full-duplex relaying (FDR) transmission sum-rate under the transmit power budget was investigated, where the self-interference channel gains were fixed, which may not be practical [25]. UAV-FDR communications have remarkable potential since it allows simultaneous data receiving and transmitting on the same channel. Hence, FDR is a preferable candidate for UAV-assisted network due to the time efficiency. This motivates us to investigate the UAV-FDR scheme, in the hope that the network throughput can be efficiently improved while UAV relay serving time can be reduced. There are few works on UAV-FDR transmissions. The most relevant work is [16], where the outage probability is minimized for full-duplex UAV that works in the decode-and-forward (DF) relaying mode. However, the authors assume that the self-interference can be eliminated completely in a relay node, which may be not realizable in practice, and energy consumption is neither taken into account.

Additionally, the UAV's intrinsic mobility feature allows the transmitters to trace the channel variations and only communicate when the channel quality becomes sufficiently good [1], [12], [14], [18]. With regard to tracing and positively exploiting the channel variations during the communications, one effective method is to apply the load-carry-and-deliver (LCAD) paradigm that was first proposed by *Cheng, et al.* in [4], [18]. Very recently, *Yong Zeng, et al.* did some innovative work on integrating LCAD into UAV HDR networks [17], [20], where only the network capacity instead of the EE is concerned. However, there are very few studies on integrating LCAD into FD relaying networks. LCAD-based FDR is particularly applicable to delay-tolerant and energy-constrained networks, where messages can be stored until the channels become better. To the best of our knowledge, it is still an open issue regarding a detailed study of *energy-efficient FD UAV-assisted mobile relaying networks*. Specifically, each transceiver works in the FD mode, and simultaneous data loading and offloading are enabled.

In this paper, we will answer two challenging questions for such a system: 1) *how to formulate the EE* that combines multiple important metrics, including signal to interference plus noise ratio (SINR) and flight power consumptions? 2) *what are the impacts of UAV flight speed on the EE?* The above two questions are critical for practical engineering implementations. Specifically, our main contributions are listed as follows:

- An FD UAV-assisted mobile relaying scheme is proposed. In particular, the self-interference complex fading coefficients follow the complex Gaussian distribution instead of being constant.
- As key metrics, the loading and offloading SINR are first analytically derived. Based on that, the cumulative distribution function (CDF) and the overall EE are formulated.
- For the FDR, the impact of the self-interference cancellation factor on the EE performance is investigated.
- The optimum flight speed is obtained by the genetic algorithm and under the information causality constraint.

The rest of the paper is organized as follows. In Section II, the system and channel model is presented. The UAV-FDR is presented in Section III. EE optimization problem formulation and analysis are given in Section IV. The genetic algorithm is applied to efficiently seek for the optimum solution, which is verified with the Brute-force method. In Section V, the numerical results are presented and analysed. The convergence behaviour is also given. Section VI concludes this paper.

Notations: The notations are listed in Table 1.

TABLE 1. Notations.

Notation	Description
$h_{ii}, i \in \{S, D, R\}$	Rayleigh fading coefficient of the self-interference loop at node i.
$h_{ij}(t), i \neq j, i, j \in \{S, D, R\}$	node i-node j free-space path-lose (FSPL) at time t.
P_i	transmitting power at node i.
$n_i \sim \mathcal{N}(0, \sigma^2)$	additive Gaussian white noise with power σ^2 at different nodes. For notation simplification, we assume the noise power is the same at different nodes, i.e. all equal to σ^2.
$x_i(t)$	unit-power transmitted signal from node i at time t.

II. SYSTEM AND CHANNEL MODEL

A. SYSTEM MODEL

A point-to-point communication in delay-tolerant device-to-device (D2D) wireless networks is studied, where two terrestrial transceivers, S and D, intend to exchange their messages. Due to the severe path loss or the presence of physical obstacles between S and D, a rotary-wing UAV flies and acts as a mobile relay to assist message exchange. The UAV works in an FDR fashion to fully exploit the relaying capacity and further improve the energy efficiency of data transmission. Specifically, we assume that each transceiver is equipped with two antennas, one for receiving and another for transmitting.

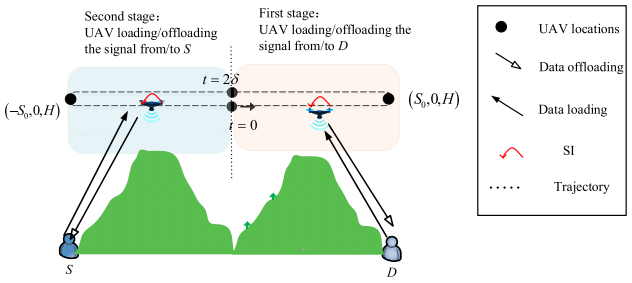

FIGURE 1. Full-duplex UAV-assisted relaying system.

As depicted in Fig. 1, a Cartesian coordinate system is considered. S and D are respectively located at $(S_0, 0, 0)$ and $(-S_0, 0, 0)$. The UAV is equipped with the global positioning system (GPS) system and can automatically finish the designed airlines as well as automatically hover in need [26]. In this paper, the FDR UAV flies horizontally at a constant altitude H and in straight lines back and forth at constant speed v, as assumed in [20]. As such, extra energy consumption due to descending/ascending operations and acceleration/deceleration can be avoided. Without loss of generality, the center, most left and right points of its trajectory are pre-set as $(0, 0, H)$, $(-S_0, 0, H)$ and $(S_0, 0, H)$, respectively.

The UAV relay serving period completing information exchange between S and D is equally divided into two stages, i.e. the first stage (FS) and second stage (SS). Each stage happens in one half-plane (see Fig. 1). We assume that it takes the UAV δ seconds to complete a one-way half-plane trip. Correspondingly, the duration of each stage and serving period are 2δ and 4δ seconds, respectively. Note that delay-tolerant UAV-assisted communications have been adopted in practice [12], [18], [27].[1] Multiple consecutive serving periods can be splited into a series of single period. The analysis for each individual period is similar. As such, we only take one period for illustrations. Note that our scenario can be also applied to a stage consisting of multiple time slots, where in each time slot, a message is delivered between S and D.

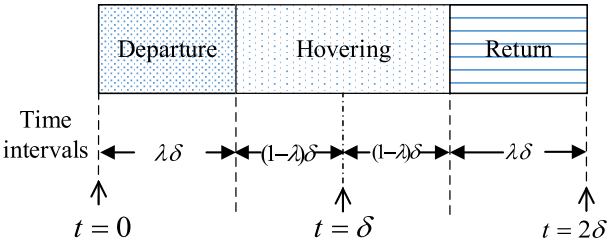

FIGURE 2. UAV flight process in the first stage.

The UAV movement in two stages are exactly symmetrical. As depicted in Fig. 2, in the departure phase of the FS, the UAV flies from $(0, 0, H)$ to $(S_0, 0, H)$. The time duration of the departure phases can be calculated as $\lambda\delta$, where $\lambda = \frac{S_0/v}{\delta}$ is the fraction of flying. If $v\delta > S_0$ (i.e. $\lambda < 1$), the UAV will be hovering at $(S_0, 0, H)$ for $2(1-\lambda)\delta$ seconds, after which the UAV flies back to $(0, 0, H)$. In case that $\lambda = 1$, the hovering phase will be skipped. During the above process, the UAV is closer to D than S. Afterwards, in the second stage (SS) (i.e. when $2\delta \leq t \leq 4\delta$), the UAV is closer to S than D. The details are omitted here.

B. CHANNEL MODEL

The UAV-to-D (or S) channel and the self-interference channels are all involved. We study the above channels as below:

[1] It has been shown that the larger delay comes at the benefit of a higher spectrum efficiency [18].

1) UAV-TO-D (OR S) CHANNEL

It can be noticed that in the first stage, when $0 \le t \le \lambda\delta$, the horizontal distance between the UAV and node D is $(S_0 - vt)$ and the UAV-to-D distance $d'_{RD}(t)$ can be obtained by $\sqrt{H^2 + (S_0 - vt)^2}$. Similarly, when $(2-\lambda)\delta \le t \le 2\delta$, the UAV flies from node D and $d'_{RD}(t)$ can be expressed as $\sqrt{H^2 + [v(t-\delta)]^2}$. Hence, we have

$$d'_{RD}(t) = \begin{cases} \sqrt{H^2 + (S_0 - vt)^2}, & 0 \le t \le \lambda\delta, \\ H, & \lambda\delta \le t \le (2-\lambda)\delta, \\ \sqrt{H^2 + [v(t-\delta)]^2}, & (2-\lambda)\delta \le t \le 2\delta. \end{cases} \quad (1)$$

The UAV channels are mainly dominated by the line-of-sight (LOS) component [14], [17], [18]. Although there may be limited multipath fading due to ground reflections, it occurs with a low probability. Furthermore, the Doppler effect due to the UAV mobility is assumed to be perfectly compensated [12], [14]. The UAV-to-D FSPL can be obtained as

$$h_{RD}(t) = \sqrt{\frac{1}{G[d'_{RD}(t)]^a}}, \quad \text{when } 0 \le t \le 2\delta, \quad (2)$$

where a denotes the path-loss exponent and $G = \frac{PL(d_0)}{d_0^a}$ is a constant used in the log-distance path loss model with $PL(d_0)$ the linear path loss at a reference distance d_0. Without loss of generality, we assume that all channels are reciprocal. In the following, without loss of generality, G is normalized to unity and a is set as $a = 2$. Let $h_m(t)$ represent the channel gain in the mth ($m \in \{1, 2, 3\}$) phase. $m = 1, 2, 3$ respectively represent the departure, hovering and phase. We have

$$h_{RD}(t) = \begin{cases} h_1(t) = \dfrac{1}{\sqrt{H^2 + (S_0 - vt)^2}}, & 0 \le t \le \lambda\delta, \\ h_2(t) = \dfrac{1}{H}, & \lambda\delta \le t \le (2-\lambda)\delta, \\ h_3(t) = \dfrac{1}{\sqrt{H^2 + [v(t-\delta)]^2}}, & (2-\lambda)\delta \le t \le 2\delta. \end{cases} \quad (3)$$

Due to the symmetry of the UAV movement in the FS and SS, UAV-to-S distance in the second stage, denoted by $d'_{SR}(t)$, can be given by

$$d'_{SR}(t) = d'_{RD}(t - 2\delta), \quad \text{when } 2\delta \le t \le 4\delta. \quad (4)$$

Correspondingly, the S-to-UAV FSPL is given as

$$h_{SR}(t) = \sqrt{\frac{1}{G[d'_{SR}(t)]^2}} \triangleq \frac{1}{d'_{SR}(t)}, \quad \text{when } 2\delta \le t \le 4\delta. \quad (5)$$

2) THE SELF-INTERFERENCE CHANNELS

Let h_{SS}, h_{DD}, h_{RR} represent the SI Rayleigh fading coefficients at node S, node D, and the UAV respectively. Assume that $|h_{RR}|^2$, $|h_{DD}|^2$, $|h_{SS}|^2$ are exponential fading power gains [25]. The probability density functions (PDFs) are denoted by, respectively,

$$\begin{aligned} f_{|h_{RR}|^2}(x) &= \frac{1}{\sigma_x^2} e^{-\frac{x}{\sigma_x^2}}, \\ f_{|h_{DD}|^2}(y) &= \frac{1}{\sigma_y^2} e^{-\frac{y}{\sigma_y^2}}, \\ f_{|h_{SS}|^2}(z) &= \frac{1}{\sigma_z^2} e^{-\frac{z}{\sigma_z^2}}, \end{aligned} \quad (6)$$

where $\sigma_x^2, \sigma_y^2, \sigma_z^2$ represent the variances of $|h_{RR}|^2$, $|h_{DD}|^2$, $|h_{SS}|^2$, respectively.

III. UAV-FDR COMMUNICATION

The LCAD scheme [18] is applied to fully exploit the channel variations. Specifically, the data will not be transmitted until the channel is advantageous (or equivalently, the UAV is closer to one node). Additionally, bidirectional communication is performed. That is, in the FS, the UAV only communicates bidirectionally with D. While in the SS, the UAV keeps communicating bidirectionally with S. Specifically, in the FS, the UAV simultaneously loads signals from D and offloads the previously received signal from S to D. In the SS, the UAV loads the signal from S while offloading the previously received signal from D to S. Based on the above analyses, 2δ also represents the data transmission delay.

In this section, we take the first stage as an example to illustrate the communication scheme. The signal model and formulations in the second stage can be obtained by exchanging "S" with "D" in the corresponding notations. The detailed offloading and loading schemes in the first stage will be respectively presented in subsections III-A and III-B.

A. DATA OFFLOADING

We assume that the amplify-and-forward (AF) policy is employed at UAV relay, which works in the full-duplex mode. Though the self-interference exists, it can be eliminated by an echo canceller [28], a phase conjugate array [29] or a retrodirective antenna [30]. Specifically, the signals received at the receiving antenna are first partially eliminated before being forwarded to the next receiving node [24].

The signal received by the UAV relay is

$$x_R(t) = \sqrt{\beta_{FS}(t)}\, y_R^{(S)}(t - 2\delta), \quad 0 \le t < 2\delta, \quad (7)$$

where $y_R^S(t - 2\delta)$ is the received signal at the UAV in the previous stage and can be represented as

$$y_R^{(S)}(t - 2\delta) = \sqrt{P_S} h_{SR}(t - 2\delta) x_S(t - 2\delta) + \sqrt{kP_R} h_{RR} x_R(t - 2\delta) + n_R, \quad (8)$$

where k is the self-interference cancellation factor, the definitions of P_S, $h_{SR}(t-2\delta)$, $x_S(t-2\delta)$, P_R, h_{RR}, $x_R(t-2\delta)$ and

n_R can be referred to Table 1 for details; $\beta_{\mathrm{FS}}(t)$ represents the power amplification factor at the UAV when it is in the FS and can be achieved as

$$\beta_{FS}(t) = \frac{P_R}{P_S\,|h_{SR}(t-2\delta)|^2 + kP_R\,|h_{RR}|^2 + \sigma^2}. \quad (9)$$

The deduction for (9) is illustrated as below. Given that the transmitting power at the UAV is P_R, it is required that the amplified signal power equal P_R, i.e.

$$\beta_{FS}(t)\mathbb{E}\{|y_R^{(S)}(t-2\delta)|^2\} = P_R, \quad (10)$$

where $\mathbb{E}\{\cdot\}$ is the expectation operator and $|z|$ means the amplitude of z. Then, by combining (8) and (10), we have (9).

The received signal at D is given as

$$y_D(t) = \sqrt{kP_D}h_{DD}x_D(t) + h_{RD}(t)\sqrt{\beta_r(t)}y_R^{(S)}(t-2\delta) + n_D, \quad \text{when } 0 \le t \le 2\delta, \quad (11)$$

where P_D is the transmitting power at node D, h_{DD} represents the Rayleigh fading coefficient of the SI loop at node D, $x_D(t)$ is the unit-power transmitted signal from D, $h_{RD}(t)$ is given in (2), n_D is the AWGN noise at D.

B. DATA LOADING

The signal received by the UAV in the FS is expressed as

$$y_{R,FS}(t) = \sqrt{P_D}h_{RD}(\mathrm{t})x_D(t) + \sqrt{kP_R}h_{RR}x_R(t) + n_R, \quad \text{when } 0 \le t \le 2\delta, \quad (12)$$

where $x_R(t)$ and n_R can be referred to Table 1 for details.

Additionally, the loading SINR, denoted as $\gamma_{load,FS}(t)$, is calculated as

$$\gamma_{load,FS}(t) = \frac{P_D\,|h_{RD}(t)|^2}{kP_R\,|h_{RR}|^2 + \sigma^2}, \text{ when } 0 \le t \le 2\delta, \quad (13)$$

where $h_{RD}(t)$ is the FSPL defined by (3).

IV. EE FORMULATION AND ANALYSIS

Note that though the UAV flight behaviour is symmetrical in the FS and SS, data offloading/loading data rates are not necessarily identical, depending on whether the transmitting power at S and D takes the same value. Hence, the EE for the whole period, instead of one stage, will be analysed in the following. We first analyse the overall energy consumption and the sum-bits, based on which the EE is formulated. The optimal flight speed maximizing the energy efficiency is also investigated.

A. ENERGY CONSUMPTION ANALYSIS

The overall energy consumption consists of UAV propulsion power consumption, communication power consumption as well as SI power consumption. We assume that the communication power consumption and SI power consumption are negligible compared to the UAV propulsion power consumption [31].

The average sum power consumption $\overline{P}_{tot}$ can be given as

$$\overline{P}_{tot} = \lambda P(v) + (1-\lambda)P_{hover}, \quad (14)$$

where $P(v)$ and P_{hover} are flying and hovering power consumptions, which are given as [31]

$$P(v) = P_0\left(1 + \frac{3v^2}{U_{tip}^2}\right) + P_i\left(\sqrt{1 + \frac{v^4}{4{v_0}^4}} - \frac{v^2}{2{v_0}^2}\right)^{1/2} + \frac{1}{2}f_0\rho sAv^3, \quad (15)$$

and

$$P_{hover} = P_0 + P_i, \quad (16)$$

respectively. To be specific, P_0 and P_i in (15) and (16) represent the blade profile power and induced power under the hovering state, respectively. They can be formulated as [31]

$$P_0 = \frac{\varepsilon}{8}\rho sA\Omega^3R_m^3, \quad P_i = (1+k_h)\frac{W^{3/2}}{\sqrt{2\rho A}}. \quad (17)$$

In (15)-(17), U_{tip}, v_0 are tip speed of the rotor and mean rotor induced velocity in the hovering state, respectively; f_0, s and ρ are the fuselage drag ratio, rotor solidity and air density, respectively; R_m is rotor radius (measured in meter); ε is profile drag coefficient; Ω is the blade angular velocity in radians; k_h is the incremental correction factor to induced power; W is the aircraft weight in Newton; and A is rotor disc area [31]. Finally, the average energy consumption can be calculated as

$$\overline{E}_{tot} = \overline{P}_{tot}4\delta = 4\delta\lambda \cdot P(v) + 4\delta(1-\lambda)\cdot P_{hover}. \quad (18)$$

B. OFFLOADING SUM-BITS DERIVATION

1) OFFLOADING SINR FORMULATION

Under the AF relaying protocol, offloading SINR is an important metric in measuring the instantaneous channel capacity. Detailed offloading SINR derivations in the FS are illustrated. The offloading SINR in the SS can be obtained by exchanging "S" with "D" in all the following notations. We ignore its details.

In the first stage, the SINR is calculated as the power of $x_S(t-2\delta)$ divided by the interference and noise power in (11). From (8) and (11), it can be obtained that the offloading SINR can be represented as

$$\gamma_{off,FS}(t) = \frac{c_1}{c_2|h_{RR}|^2 + c_3|h_{DD}|^2 + c_4|h_{RR}|^2|h_{DD}|^2 + c_5}, \quad \text{when } 0 \le t \le 2\delta, \quad (19)$$

where

$$\begin{aligned} c_1 &= P_RP_S|h_{RD}(t)|^2|h_{SR}(t-2\delta)|^2,\\ c_2 &= |h_{RD}(t)|^2kP_R{}^2 + kP_R\sigma^2,\\ c_3 &= |h_{SR}(t-2\delta)|^2kP_DP_S + kP_D\sigma^2,\\ c_4 &= k^2P_DP_R,\\ c_5 &= P_R|h_{RD}(t)|^2\sigma^2 + \sigma^2P_S|h_{SR}(t-2\delta)|^2 + \sigma^4. \end{aligned} \quad (20)$$

The rate on the $D-to-UAV$ channel is

$$C_{off,FS} = B\log(1+\gamma_{off,FS}(t)), \quad 0 \le t \le 2\delta, \quad (21)$$

where B is the bandwidth.

An outage event occurs on the $S-to-UAV$ or $D-to-UAV$ channel when the fixed data transmission rate R_0 is larger than the achievable rate. Let $\theta=2^{R_0/B}-1$ and the probability that the $D-to-UAV$ offloading SINR is less than θ can be calculated by

$$\Pr_{out}=\{\gamma_{off,FS}<\theta\}. \tag{22}$$

Then the CDF of $C_{off,FS}$ can be expressed as

$$F_1(\theta)=e^{-\frac{c_{dd}}{\sigma_y^2}}+\int_0^{c_{dd}}\frac{1}{\sigma_y^2}e^{-\frac{y}{\sigma_y^2}}e^{-\frac{c_6-c_3y}{c_4\sigma_x^2y+c_2\sigma_x^2}}dy, \tag{23}$$

where $y=|h_{DD}|^2$, $c_6=c_1/\theta-c_5$, $c_{dd}=\frac{c_1/\theta-c_5}{c_3}$ (i.e., the solution of $\frac{c_1}{\theta}-c_5-c_3y=0$).

Proof: Please refer to Appendix A.

2) ACCUMULATED OFFLOADING SUM-BITS

Let $A_{\Sigma_{off,FS}}$ represent the sum bits of data offloading when the UAV is in flying and hovering states in the FS,

$$A_{\sum off,FS}=\int_0^{2\delta}(1-F_1(\theta))R_0dt. \tag{24}$$

Let $A_{\Sigma_{off,SS}}$ represent the sum bits of data offloading when the UAV is in flying and hovering states in the SS.

$$A_{\sum off,SS}=\int_{2\delta}^{4\delta}(1-F_2(\theta))R_0dt, \tag{25}$$

where $F_2(\theta)$ is the offloading CDF in SS states, which can be obtained by exchanging "P_S" with "P_D".

Correspondingly, the final sum-bits in one complete period are

$$A_\Sigma=A_{\sum off,FS}+A_{\sum off,SS}. \tag{26}$$

C. LOADING SUM-BITS DERIVATION

The CDF of $\gamma_{load,FS}$ in the FS can be expressed as

$$F_{load1}(\theta)=e^{-\frac{\frac{P_D|h_{RD}(t)|^2}{\theta}-\sigma^2}{kP_R\sigma_x^2}}. \tag{27}$$

Proof: Please refer to Appendix B.

Let $A_{\Sigma_{load,FS}}$ represent the sum bits of data offloading when the UAV is in flying and hovering states in the FS,

$$A_{\sum load,FS}=\int_0^{2\delta}(1-F_{load1}(\theta))R_0dt. \tag{28}$$

Let $A_{\Sigma_{off,SS}}$ represent the sum bits of data offloading when the UAV is in flying and hovering states in the SS.

$$A_{\sum off,SS}=\int_{2\delta}^{4\delta}(1-F_{load2}(\theta))R_0dt, \tag{29}$$

where $F_{load2}(\theta)$ is the offloading CDF in SS states, which can be obtained by exchanging "S" with "D".

D. EE OPTIMIZATION PROBLEM FORMULATION AND SOLVING

Based on the above derivations, the resulting EE can be finally expressed by

$$\eta_{EE}=\frac{A_\Sigma}{E_{tot}}. \tag{30}$$

We aim at determining the EE-optimum v. The information causality has to be satisfied, i.e. the total number of loaded bits in one stage shall be no larger than that of being offloaded in the next stage. To be specific, on one hand, we require that the bit number loaded from S in one stage (i.e. when UAV is in the left-half plane) shall be no less than that of being offloaded in the next stage (i.e. when UAV is in the right-half plane). Hence, the constraint (31) has to be satisfied.

$$A_{\sum off,FS}\le A_{\sum load,SS}, \tag{31}$$

$$A_{\sum off,SS}\le A_{\sum load,FS}. \tag{32}$$

On the other hand, we require that the number of bits loaded from D in one stage (i.e. when the UAV is in the FS) shall be no less than that of being offloaded to S in the next stage. Hence, the constraint (32) must be satisfied.

The optimization problem can be formulated as

$$\mathbf{P1}:\ v^*=\underset{v}{\operatorname{argmax}}\ \eta_{EE} \tag{33}$$

$$s.t.\quad v\le v_{\max},$$

$$(31),\ (32), \tag{34}$$

where $(\cdot)^*$ represents the optimum solution, $v_{\max}$ represents the maximum speed and is a constant.

Next, the genetic algorithm [32] is applied. Its basic idea is to create a set of candidate speed strategies, and allow them to evolve through crossover and mutation, so that the speed strategy can develop towards a better solution, and can gradually approach the optimal solution. A chromosome is defined as the vector of flight velocity, i.e. $\mathbb{C}^{1\times M}=[v_1,v_2,\cdots,v_M]$, where M is the length of a chromosome. A population is the set of chromosomes. Under the constraints (31) and (32), we obtain the solution of (**P1**).

V. NUMERICAL RESULTS

In this section, we provide the analytical results and investigate the impact of v on the EE. Additionally, the EE under the FDR scheme will be compared with those under the HDR as well as static-relaying schemes.

The parameter settings are applicable to practical engineering implementations and given in Table 2, unless otherwise specified. Note that the settings of parameters in (15)-(17) are provided in [31].

A. IMPACT OF v ON THE EE

The channel capacity that includes both data loading and offloading capacity in the FDR scheme is first demonstrated. Fig. 3 presents the channel capacity curves versus t. It is shown that the channel capacity increases until the UAV arrives at point $(S_0, 0, H)$, where the UAV hovers and channel

TABLE 2. Parameter settings.

Parameters	Value	Parameters	Value
H	100 m	S_0	1000 m
P_S	0.2 W	$P_D = P_R$	0.1 W
k	0.001	B	10 MHz
R_0	10^6	δ	50 s
σ_x^2	0.1	σ_y^2	0.1
ε	0.012	ρ	1.125
Ω	400	σ^2	-120 dB
k_h	0.1	W	400
A	0.79	s	0.05
U_{tip}	200	v_0	7.3
f_0	0.3	R_m	0.5 W
a	2	G	1

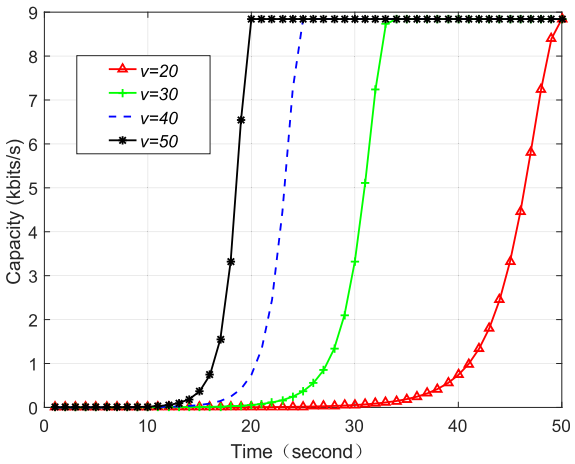

FIGURE 3. Channel capacity under FDR at different speeds (m/s); $0 \le t \le \delta$; $2\delta = 100$s.

gain remains unchanged. It also shows that the larger the UAV speed is, the sooner it reaches the hovering point, which is reasonable.

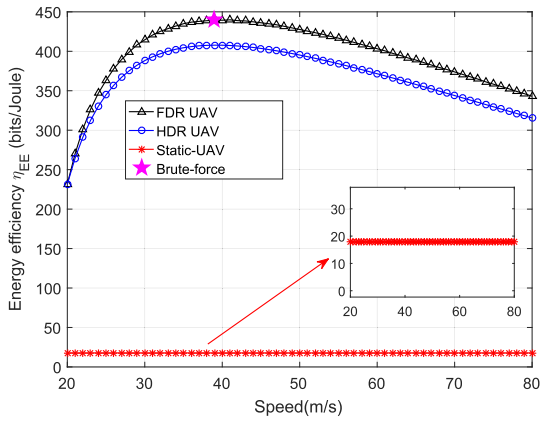

FIGURE 4. UAV energy efficiency under different schemes.

Furthermore, to investigate the impact of v on the EE and verify the advantage of the FDR scheme, we also present the EE curves versus v under the HDR as well as static schemes in Fig. 4. For the static model, data loading and offloading are

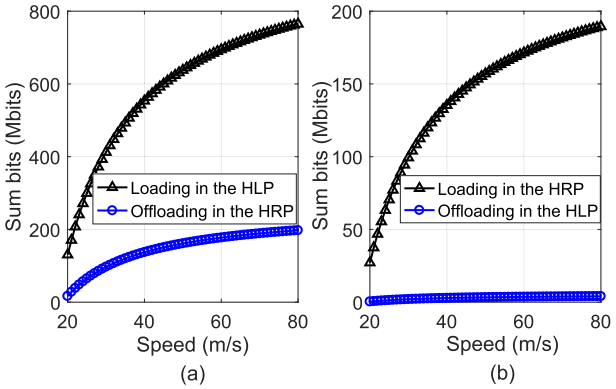

FIGURE 5. UAV sum loading/offloading bits on the FS and SS. In (*a*), pre-SS represents the SS in the previous period, while cur-FS resprents the FS in the current period.

simultaneously performed at point (0, 0, H). For HDR model, the UAV loads data from D in the FS and offloads data to S in the SS.

Let η_{HDR} and η_{static} respectively represent the EE under the HDR as well as static schemes. The following observations can be obtained. Firstly, the Brute-force (BF) searching results reveal that $\eta_{EE} > \eta_{HDR} \gg \eta_{static}$, which indicates that our FDR scheme outperforms the others in terms of the EE. v^*, the optimal solution obtained by the BF, is marked with a star in Fig. 4. Compared with the half-duplex system where the UAV only loads information in the half-plane, the full-duplex system is more energy-saving because of its higher transmission rate which leads to a smaller transmission duration and saves much energy for flight. Additionally, we can see that constraints (31) and (32) are respectively demonstrated in Figs. 5(a) and (b). Clearly, the constraints are satisfied. Furthermore, the EE under the FDR scheme first sharply increases with v until it reaches the maximum value at $v = 38.985$ m/s; afterwards, it falls. The underlying reason can be analysed as follows: as v increases, the UAV arrives at the hovering point earlier, and stays there for a larger time proportion, where data loading and offloading experiences the best channel gains, such that the average channel capacity is significantly improved. However, as v substantially increases, the offloading data bit number increases gently as depicted in Fig. 5, while the average flight power consumption increases abruptly, which comprehensively leads to a degraded EE.

The convergence curve is also presented in Fig. 6, where the resulting optimal energy efficiency is 439.99 bits/joule and the corresponding speed is around 38 m/s. The result closely matches with the maximum η_{EE} obtained by the Brute-force. Hence, the validity of the genetic algorithm is proved. Besides, the iteration stops at the 10th generation (namely, 10 iteration times), which shows that the curve converges very quickly.

Furthermore, the EEs when the UAV hovering in different positions were compared. That is, the UAV simply hovers at the middle point between D and S, over node D or node S.

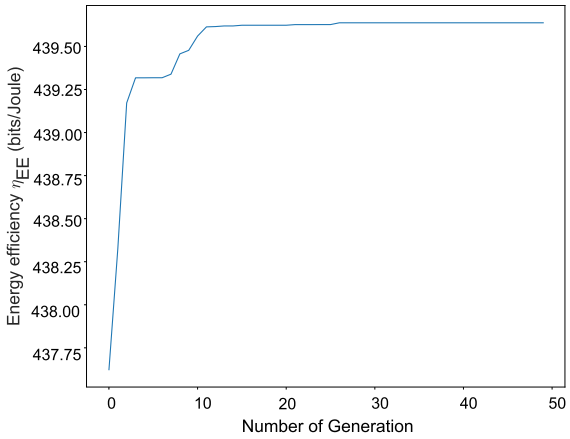

FIGURE 6. UAV energy efficiency curve under FDR with the genetic algorithm.

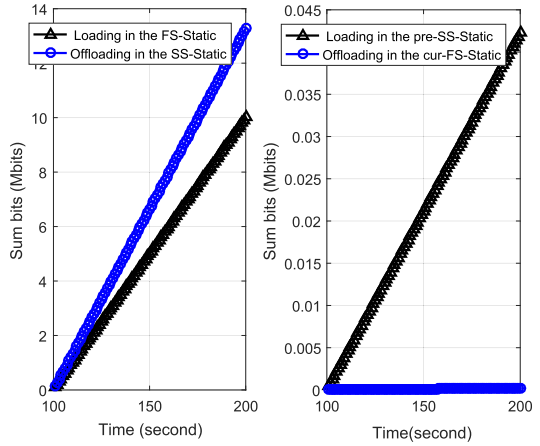

FIGURE 7. Static sum loading/offloading bit number in the FS and SS. In (*b*), pre-SS represents the SS in the previous period, while cur-FS represents the FS in the current period.

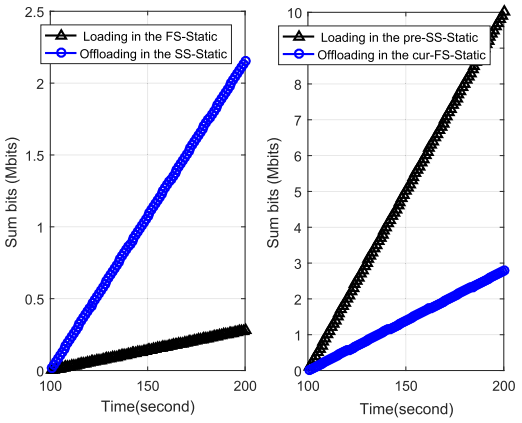

FIGURE 8. Static sum loading/offloading bit number in the FS and SS. In (*b*), pre-SS represents the SS in the previous period, while cur-FS represents the FS in the current period.

However, the model where the UAV hovers over node D or S does not satisfy the information causality constraint (See Fig. 7 and Fig. 8).

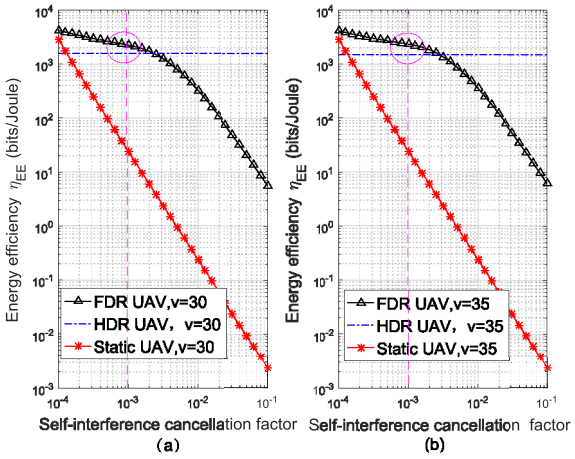

FIGURE 9. UAV energy efficiency under different self-interference cancellation factors. (a) $v = 30$ m/s, (b) $v = 35$ m/s.

B. IMPACT OF SELF-INTERFERENCE CANCELLATION FACTOR ON THE EE

To investigate the impact of the self-interference cancellation factor k on the EE and verify the advantage of the FDR scheme, we present the EE curves versus k for two different speed scenarios (i.e., $v = 30$ m/s, $v = 35$ m/s) in Fig. 9. For the static model, data loading and offloading are simultaneously performed at point $(0, 0, H)$. For the HDR model, the UAV loads data from D in the FS and offloads data to S in the SS.

It is first observed that the energy efficiency under the FDR model decreases with k. On the other hand, compared with the Static-FDR model, the UAV-FDR model decreases slowly, which shows that our FDR scheme outperforms the others in terms of the EE.

In addition, it can be noticed that the HDR performs better when k approaches 10^{-2}. Note that in practice, k can be smaller than 10^{-3} with the current self-interference cancellation technique [28]–[30]. Fig. 4 shows that when $k = 0.001$, the EE of FDR is about 450 bits/joule and performs better than the HDR.

VI. CONCLUSIONS

An energy-efficient full-duplex UAV relaying network has been studied for the delay-tolerant networks. The load-carry-and-delivery scheme has been applied to positively take advantage of the variations of the channel gains. Additionally, the self-interference channel gains were considered to be random and follow the complex Gaussian distribution. Numerical results demonstrated that the proposed scheme outperforms the half-duplex as well as static schemes.

The optimum flight speed has been obtained to maximize the EE by the genetic algorithm and under the information causality constraint. The validity of the genetic algorithm has been illustrated and the convergence behavior has also been demonstrated. Finally, it has been shown that EE decreases with the self-interference cancellation.

APPENDIX

A. CALCULATIONS OF (23)

The CDF of $\gamma_{off,FS}$ in the FS can be expressed as

$$\begin{aligned} F_1(\theta) &= \Pr\left\{\frac{c_1}{c_2|h_{RR}|^2 + c_3|h_{DD}|^2 + c_4|h_{RR}|^2|h_{DD}|^2 + c_5} < \theta\right\} \\ &= 1 - \Pr\left\{|h_{RR}|^2 \le \frac{\frac{c_1}{\theta} - c_5 - c_3|h_{DD}|^2}{c_2 + c_4|h_{DD}|^2}\right\}. \end{aligned} \tag{35}$$

Let $x = |h_{RR}|^2$. Recall that $y = |h_{DD}|^2$, we have

$$\Pr\left\{x \le \frac{\frac{c_1}{\theta} - c_5 - c_3 y}{c_2 + c_4 y}\right\} = \int_0^{c_{dd}} \frac{1}{\sigma_y^2} e^{-\frac{y}{\sigma_y^2}} \int_0^{g_d^{up}} \frac{1}{\sigma_x^2} e^{-\frac{x}{\sigma_x^2}} dx dy, \tag{36}$$

where $g_d^{up} = \frac{\frac{c_1}{\theta} - c_5 - c_3|h_{DD}|^2}{c_2 + c_4|h_{DD}|^2}$, c_{dd} is given below (23). Then (36) is rewritten as

$$\begin{aligned} \Pr\left\{x \le \frac{\frac{c_1}{\theta} - c_5 - c_3 y}{c_2 + c_4 y}\right\} &= 1 - e^{-\frac{c_{dd}}{\sigma_y^2}} \\ &\quad - \int_0^{c_{dd}} \frac{1}{\sigma_y^2} e^{-\frac{y}{\sigma_y^2}} e^{-\frac{c_6 - c_3 y}{c_4\sigma_x^2 y + c_2\sigma_x^2}} dy, \end{aligned} \tag{37}$$

where c_6 is given below (23).

From (35), (37), the offloading $D - to - UAV$ CDF can be expressed as (23).

B. CALCULATIONS OF (27)

The CDF of $\gamma_{load,FS}$ in the FS can be expressed as

$$\begin{aligned} F_{load1}(\theta) &= \Pr\left\{\frac{P_D\,|h_{RD}(t)|^2}{kP_R\,|h_{RR}|^2 + \sigma^2} < \theta\right\} \\ &= 1 - \Pr\left\{|h_{RR}|^2 \le \frac{\frac{P_D|h_{RD}(t)|^2}{\theta} - \sigma^2}{kP_R}\right\}, \end{aligned} \tag{38}$$

where the FSPLA $h_{RD}(t)$ is defined by (3). Let $x = |h_{RR}|^2$. Note that

$$\Pr\left\{x \le \frac{\frac{P_D|h_{RD}(t)|^2}{\theta} - \sigma^2}{kP_R}\right\} = 1 - e^{-\frac{\frac{P_D|h_{RD}(t)|^2}{\theta} - \sigma^2}{kP_R\sigma_x^2}}. \tag{39}$$

From (38), (39), the loading $D - to - UAV$ CDF can be expressed as (27).

REFERENCES

[1] L. Gupta, R. Jain, and G. Vaszkun, "Survey of important issues in UAV communication networks," *IEEE Commun. Surveys Tuts.*, vol. 18, no. 2, pp. 1123–1152, 2nd Quart., 2016.

[2] A. Carrascocasado, R. Vergaz, and M. Josánchez Pena, "Design and early development of a UAV terminal and a ground station for laser communications," *Proc. SPIE, Int. Soc. Optical Eng.*, vol. 8184, no. 4, p. 361, 2011.

[3] J. Tang, L. Fan, and S. Lao, "Collision avoidance for multi-UAV based on geometric optimization model in 3D airspace," *Arabian J. Sci. Eng.*, vol. 39, no. 11, pp. 8409–8416, Oct. 2014.

[4] C.-M. Cheng, P.-H. Hsiao, H. T. Kung, and D. Vlah, "Maximizing throughput of UAV-relaying networks with the Load-Carry-and-Deliver paradigm," in *Proc. IEEE Wireless Commun. Netw. Conf.*, Mar. 2007, pp. 4417–4424.

[5] [Online]. Available: https://spectrum.ieee.org/automaton/consumer-electronics/gadgets/mit-builds-drone-based-rfid-relay-to-track-boxes-in-warehouses

[6] S. Kota and G. Giambene, "Satellite 5G: IoT use case for rural areas applications," in *Proc. 11th Int. Conf. Adv. Satellite Space Commun.*, 2019, pp. 24–28.

[7] [Online]. Available: http://alpine-robotics.com/projects/future/flying-relay-station/

[8] [Online]. Available: https://dronerush.com/product/parrot-anafi/

[9] [Online]. Available: https://dronerush.com/yuneec-drones-guide-wind-9821/

[10] [Online]. Available: https://dronerush.com/product/dji-mavic-2-zoom/

[11] N. Qi, "M. Xiao, T. A. Tsiftsis, L. Zhang, M. Skoglund, and H. Zhang, "Efficient coded cooperative networks with energy harvesting and transferring," *IEEE Trans. Wireless Commun.*, vol. 16, no. 10, pp. 6335–6349, Jul. 2017.

[12] Q. Wu, Y. Zeng, and R. Zhang, "Joint trajectory and communication design for multi-UAV enabled wireless networks," *IEEE Trans. Wireless Commun.*, vol. 17, no. 3, pp. 2109–2121, Mar. 2018.

[13] W.-J. Wang and H.-C. Yang, "Effect of imperfect spectrum sensing on slotted secondary transmission: Energy efficiency and queuing performance," *IEEE Trans. Cognit. Commun. Netw.*, vol. 4, no. 4, pp. 764–772, Dec. 2018.

[14] Y. Zeng and R. Zhang, "Energy-efficient UAV communication with trajectory optimization," *IEEE Trans. Wireless Commun.*, vol. 16, no. 6, pp. 3747–3760, Jun. 2017.

[15] C. Zhan, Y. Zeng, and R. Zhang, "Energy-efficient data collection in UAV enabled wireless sensor network," *IEEE Wireless Commun. Lett.*, vol. 7, no. 3, pp. 328–331, Jun. 2018.

[16] M. Hua, Y. Wang, Z. Zhang, C. Li, Y. Huang, and L. Yang, "Outage probability minimization for low-altitude UAV-enabled full-duplex mobile relaying systems," *China Commun.*, vol. 15, no. 5, pp. 9–24, May 2018.

[17] Y. Zeng, R. Zhang, and T. J. Lim, "Throughput maximization for UAV-enabled mobile relaying systems," *IEEE Trans. Commun.*, vol. 64, no. 12, pp. 4983–4996, Dec. 2016.

[18] Y. Zeng, R. Zhang, and T. J. Lim, "Wireless communications with unmanned aerial vehicles: Opportunities and challenges," *IEEE Commun. Mag.*, vol. 54, no. 5, pp. 36–42, May 2016.

[19] S. Zhang, H. Zhang, Q. He, K. Bian, and L. Song, "Joint trajectory and power optimization for UAV relay networks," *IEEE Commun. Lett.*, vol. 22, no. 1, pp. 161–164, Jan. 2018.

[20] J. Zhang, Y. Zeng, and R. Zhang, "Spectrum and energy efficiency maximization in UAV-enabled mobile relaying," in *Proc. IEEE Int. Conf. Commun. (ICC)*, May 2017, pp. 1–6.

[21] Z. Zhang, Z. Ma, Z. Ding, M. Xiao, and G. K. Karagiannidis, "Full-duplex two-way and one-way relaying: Average rate, outage probability, and tradeoffs," *IEEE Trans. Wireless Commun.*, vol. 15, no. 6, pp. 3920–3933, Feb. 2016.

[22] I. Krikidis, H. A. Suraweera, P. J. Smith, and C. Yuen, "Full-duplex relay selection for amplify-and-forward cooperative networks," *IEEE Trans. Wireless Commun.*, vol. 11, no. 12, pp. 4381–4393, Dec. 2012.

[23] T. Riihonen, S. Werner, and R. Wichman, "Comparison of full-duplex and half-duplex modes with a fixed amplify-and-forward relay," in *Proc. IEEE Wireless Commun. Netw. Conf.*, Apr. 2009, pp. 1–5.

[24] H. Wang, J. Wang, G. Ding, J. Chen, Y. Li, and Z. Han, "Spectrum sharing planning for full-duplex UAV relaying systems with underlaid D2D communications," *IEEE J. Sel. Areas Commun.*, vol. 36, no. 9, pp. 1986–1999, Sep. 2018.

[25] L. Zhang, J. Liu, M. Xiao, G. Wu, Y.-C. Liang, and S. Li, "Performance analysis and optimization in downlink NOMA systems with cooperative full-duplex relaying," *IEEE J. Sel. Areas Commun.*, vol. 35, no. 10, pp. 2398–2412, Oct. 2017.

[26] [Online]. Available: https://dronerush.com/yuneec-drones-guide-wind-9821/

[27] W. Zhao, M. Ammar, and E. Zegura, "A message ferrying approach for data delivery in sparse mobile ad hoc networks," in *Proc. 5th ACM Int. Symp. Mobile ad hoc Netw. Comput. (MobiHoc)*, 2004, pp. 187–198.

[28] S. Chen, M. A. Beach, and J. P. McGeehan, "Division-free duplex for wireless applications," *Electron. Lett.*, vol. 34, no. 2, p. 147, 1998.

[29] Y. Chang, H. R. Fetterman, I. L. Newberg, and S. K. Panaretos, "Microwave phase conjugation using antenna arrays," *IEEE Trans. Microw. Theory Techn.*, vol. 46, no. 11, pp. 1910–1919, Nov. 1998.
[30] B. Z. Wang, W. Wu, C. Yu, and S. Xiao, "A compact retrodirective wire antenna with two isolated ports," in *Proc. IEEE Antennas Propag. Soc. Int. Symp.*, Jun. 2003, pp. 316–319.
[31] Y. Zeng, J. Xu, and R. Zhang, "Energy minimization for wireless communication with rotary-wing UAV," *IEEE Trans. Wireless Commun.*, vol. 18, no. 4, pp. 2329–2345, Mar. 2019.
[32] X. Liu, Y. Liu, and Y. Chen, "Deployment and movement for multiple aerial base stations by reinforcement learning," in *Proc. IEEE Globecom Workshops (GC Wkshps)*, Dec. 2018, pp. 1–6.

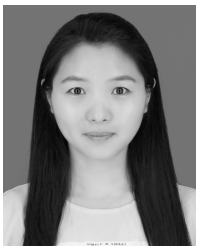

NAN QI (Member, IEEE) received the B.Sc. and Ph.D. degrees in communications engineering from Northwestern Polytechnical University (NPU), China, in 2011 and 2017, respectively. From 2013 to 2015, she was a Visiting Scholar with the Department of Electrical Engineering, KTH Royal Institute of Technology, Sweden. She is currently an Assistant Professor with the Department of Electronic Engineering, Nanjing University of Aeronautics and Astronautics, China. Her research interests include UAV-assisted communications, mobile edge computing, wireless network protocol design, optimization of wireless communications, network coding, cooperative relaying networks, and wireless energy harvesting and transferring systems.

MEI WANG received the B.S. degree in electronic information science and technology from Nanjing Agricultural University, Nanjing, China, in 2018. She is currently pursuing the M.S. degree in signal and information processing with the Nanjing University of Aeronautics and Astronautics.

WEN-JING WANG (Member, IEEE) received the Ph.D. degree in electrical and computer engineering from the University of Victoria, Victoria, BC, Canada, in 2019. He is currently with the School of Communication and Information Engineering, Xi'an University of Posts and Telecommunications. His research interests include cognitive ratio, energy efficient communications, system performance analysis, and optimization.

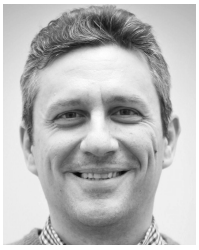

THEODOROS A. TSIFTSIS (Senior Member, IEEE) was born in Lamia, Greece, in 1970. He received the B.Sc. degree in physics from the Aristotle University of Thessaloniki, Greece, in 1993, TSIFTSIS the M.Sc. degree in digital systems engineering from the Heriot-Watt University, Edinburgh, U.K., in 1995, the M.Sc. degree in decision sciences from the Athens University of Economics and Business, in 2000, and the Ph.D. degree in electrical engineering from the University of Patras, Greece, in 2006. He is currently a Professor with the School of Intelligent Systems Science and Engineering, Jinan University, Zhuhai, China, and also an Honorary Professor with Shandong Jiaotong University, Jinan, China. His research interests include the broad areas of cognitive radio, communication theory, wireless powered communication systems, optical wireless communication, and ultra-reliable low-latency communication.

Prof. Tsiftsis has been appointed to a two year term as the IEEE Vehicular Technology Society Distinguished Lecturer (IEEE VTS DL), Class 2018. He has served as a Senior or an Associate Editor in the Editorial Boards for the IEEE TRANSACTIONS ON VEHICULAR TECHNOLOGY, the IEEE COMMUNICATIONS LETTERS, the *IET Communications*, and the IEICE TRANSACTIONS ON COMMUNICATIONS. He is currently an Area Editor for Wireless Communications II of the IEEE TRANSACTIONS ON COMMUNICATIONS and an Associate Editor of the IEEE TRANSACTIONS ON MOBILE COMPUTING.

RUGUI YAO (Senior Member, IEEE) received the B.Sc., M.Sc., and Ph.D. degrees in telecommunications and information systems from the School of Electronics and Information (SEI), Northwestern Polytechnical University (NPU), Xi'an, China, in 2002, 2005, and 2007, respectively. From 2007 to 2009, he worked as a Postdoctoral Fellow with NPU. Since 2009, he has been with SEI, NPU, Xi'an, China, where he is currently a Full Professor. In 2013, he joined ITP Laboratory, Georgia Tech, Atlanta, USA, as a Visiting Scholar. He has worked in the areas of physical layer security, cognitive radio networks, channel coding, OFDM transmission, and spread-spectrum systems. He is a Senior Member of the Chinese Institute of Electronics and China Institute of Communications.

GUANGHUA YANG (Senior Member, IEEE) received the Ph.D. degree in electrical and electronic engineering from the University of Hong Kong, Hong Kong, in 2006. From 2006 to 2013, he was a Postdoctoral Fellow, a research Associate, and a Project Manager with the University of Hong Kong. Since April 2017, he has been an Associate Professor and an Associate Dean with the Institute of Physical Internet, Jinan University, Guangdong, China. His research interests are in the general areas of communications, networking and multimedia.